Placental Image Analysis using Coupled Diffusion-Weighted and Multi-Echo T2 MRI and a Multi-Compartment Model

Andrew Melbourne[1], Rosalind Pratt[2], David Owen[1], Magdalena Sokolska[3], Alan Bainbridge[3], David Atkinson[4], Giles Kendall[2], Jan Deprest[5], Tom Vercauteren[1], Anna David[2], and Sebastien Ourselin[1]

[1]Centre for Medical Image Computing, University College London, UK. [2]Institute for Women's Health, University College Hospital, London, UK . [3]Medical Physics, University College Hospital, London, UK. [4]Centre for Medical Imaging, University College London, UK. [5]University Hospital KU Leuven, Belgium

Abstract. Current popular methods of flow and fluid measurement are confounded by the interaction of relaxation and perfusion characteristics which are rarely simultaneously considered. To address this shortcoming we propose a new multi-compartment model for the tissue signal in MRI and apply this to placenta imaging data. Motivated by the different flow characteristics across the placenta, a three compartment model comprising fast and slowly circulating fluid pools and a tissue pool is fitted to overlapping multi-echo T2 relaxometry and an intra-voxel incoherent motion diffusion acquisition with low b-values. The new model is supported by a modified image acquisition to enable successful model fitting, but this acquisition is clinically practical; we implemented the acquisition on a standard 1.5T clinical system with acquisition taking less than 20 minutes with 26 slices. This is particularly important for placenta image acquisition. We test this combined acquisition and model-fitting routine on simulated data and show parametric maps for a placenta dataset.

1 Introduction

Monitoring placental function using magnetic resonance imaging (MRI) is a growing research area [1]. Several modalities from MRI have been investigated for monitoring placental blood flow and function, each with their own advantages and disadvantages [2, 3]. Of these techniques, diffusion weighted imaging (DWI) is becoming increasingly widespread in abdominal and placental imaging. When combined with the intra-voxel incoherent motion model (IVIM[4]) of blood flow in capillaries, it provides a non-invasive method of measuring tissue properties relating to flow and perfusion. T2 relaxometry, made possible by the acquisition of images with variable echo-time, provides additional information on the static tissue composition and the intrinsic tissue T2 value. Both techniques have been proposed for placental imaging [5, 6] but how best to measure the microstructural and microvascular properties of placental tissue remains an open question. T2 relaxometry has been used specifically for monitoring placenta of

small for gestational age (SGA) fetuses and given the effect size observed between SGA and appropriate for GA pregnancies, is likely to have wider application for assessing placental function in a range of other conditions [6]. IVIM has also been measured in the placenta of SGA pregnancies and found to correlate well with measures from uterine artery Doppler ultrasound [5]. The effects seen using both IVIM and T2 relaxometry are dependent upon one another and how they are acquired, and with separate studies it will be difficult to isolate changes to the structural T2 measurement from the functional flow measurement of IVIM. To address this problem, we outline a three-compartment model that combines IVIM modelling and T2 relaxometry to measure these emergent markers of underlying microvascular properties. In the case of the placenta, we speculate that this model can be used to characterise differences between rapid and slow circulation, which we theorise may be used to represent regional vascular differences between fetal and maternal circulations.

2 Methods

2.1 Data

We obtained free-breathing data from a single subject on a 1.5T Siemens Symphony. We obtained IVIM measurements at seven b-values [0,50,100,150,200, 400,600]$s.mm^{-1}$and T2 relaxometry measurements at 9 echo times [77,90,120,150, 180,210,240,270,300]ms at resolution $1.9 \times 1.9 \times 6mm$. The b-value increments and shortest TE were fixed by the MR scanner. In addition we obtained T2 relaxometry measurements at the same 9 echo times with a diffusion b-value of $200s.mm^{-2}$ to better separate long T2 compartments with different incoherent motion properties. The total acquisition time was about 20 minutes (including localisation) making it tolerable for subjects. All images were acquired with the same echo-planar read-out and the TR was held at $3900ms$ but allowed to lengthen for longer TE measurements. Because of typical abdominal T1 values, differences in signal due to variable TR are expected to be less than 1% and the effect of otherwise lengthening the scan using fixed TR will reduce its clinical utility. The subject was pregnant with monochorionic-diamniotic twins at around 26 weeks gestation having had successful surgery for twin-twin transfusion four weeks prior. To minimise the effect of non-rigid abdominal motion we used an open-source non-rigid registration routine [7, 8] and manually segmented organs of interest. The study was approved by the local research ethics committee and the subject gave written informed consent.

2.2 Single-component signal modelling

Single component models, especially those that are mono exponential, are widespread in MRI and often used immediately by the machine software to generate parametric maps. Fitting of these models is usually carried out by using either a log-linearised signal model, or by using a non-linear algorithm to fit directly for the

parameters of interest. For diffusion MRI the parameter of interest is normally the apparent diffusion coefficient (ADC, d_{adc}) within the mono-exponential (1):

$$S(b) = S_0^* e^{-bd_{adc}} \tag{1}$$

with initial signal magnitude S_0^* (implicitly absorbing T2 signal decay), as a function of b-value b. Whilst for relaxometry the parameter of interest is the T2 rate itself (or its inverse, the relaxivity r_2) within a signal that is a function of echo-time t, with an initial signal magnitude S_0 (2):

$$S(t) = S_0 e^{-tr_2} \tag{2}$$

In principle, these parameters may be estimated simultaneously, requiring a minimum of three images to fit the three unknown parameters (S_0, d_{adc}, r_2) (3):

$$S(b,t) = S_0 e^{-bd_{adc}-tr_2} \tag{3}$$

2.3 Two-component signal modelling

Two-compartment models for diffusion and relaxometry are well established. Intra-Voxel Incoherent Motion (IVIM) is used to simultaneously model perfusion and diffusion using DWI, whilst distinct exponential decays are used in multi-compartment relaxometry to describe, for instance, fluid and non-fluid components.

IVIM Modelling The IVIM model [4] attempts to describe a tissue fluid pool that, due to the arbitrary arrangement of local capillaries, resembles enhanced diffusion. This vascular circulation can be modelled as a separate contribution to the ordinary mono-exponential diffusion, and is visible at low b-value. Equation 4 describes two components in terms of the initial signal magnitude S_0^* (again with implicit T2 decay), the vascular density (IVIM volume fraction), f_{ivim}, and two diffusivities, d^*_{ivim} and d, of the IVIM and ordinary diffusion coefficients respectively, given a set of experimental b-values, $\mathbf{b}$.

$$S(b) = S_0^* \left[f_{ivim} e^{-\mathbf{b}d^*_{ivim}} + (1 - f_{ivim}) e^{-\mathbf{b}d} \right] \tag{4}$$

Since measurements by diffusion imaging typically have low SNR, direct parameter estimation of (4) is quite difficult and prone to local minima. More robust measurements can be made by first fitting the ordinary apparent diffusion coefficient (ADC) to data with b-value greater than $100 s.mm^{-1}$ and holding this fixed whilst the remaining three parameters are fitted using nonlinear least squares (LSQ) with the constraints that $S_0^* \geq 0$, $0 \leq f_{ivim} \leq 1$ and $d^*_{ivim} > d$.

Two-component relaxometry Single- and multi-component T2 relaxometry are widely used to quantify underlying tissue properties [9] especially in neuroimaging where it can be used to estimate the relative contribution of myelin to the voxel signal. In this work we make the assumption that there are at most two T2

components in our organs of interest: one with a long T2 corresponding to a fluid pool; and one with a short T2 relating to the static tissue. Typically abdominal T2 values at 1.5T from [10] are $290 \pm 30ms$ for blood and $46 \pm 6ms$ for liver. Equation 5 describes such a two compartment model represented by relaxivities ($T2 = 1/r_2$) for blood r_2^b and tissue component r_2^t, weighted by blood-pool volume fraction, ν, given a set of experimental TEs, $\mathbf{t}$.

$$S(t) = S_0 \left[\nu e^{-tr_2^b} + (1-\nu) e^{-tr_2^t} \right] \tag{5}$$

The four parameters can be fitted using a standard non-linear least squares routine, or if r_2^b and r_2^t are assumed to be known [10], the model becomes one that is linear in the two parameters S_0 and ν. The two compartments in the T2 relaxometry model (5) are only equivalent to those in the IVIM model (4) if the long T2 pool is considered to be entirely undergoing IVIM and the short T2 pool represents static tissue only.

2.4 Three-component signal modelling

The two compartments of the IVIM model, f_{ivim}, and T2 relaxometry model, ν, will not in general be equivalent. IVIM is sensitive to a band of pseudo-diffusivities, whilst T2 relaxometry compartments are not explicitly sensitive to motion. If there are measurable static and flowing blood (or fluid) pools, f_{ivim} and ν will diverge, for instance in cystic regions (see Figure 1). The general model below combines the effects of T2 relaxation and diffusion-weighting and has up to seven free parameters, although it is possible to simplify the fitting by fixing values of d, r_2^b and r_2^t and fit for the remaining four parameters, which we do in this work. $f_{joint} \neq f_{ivim}$ as a result of enforcing multi-T2 decay which attributes the signal decay to two different processes rather than one.

$$S(b,t) = S_0 \big[f_{joint} e^{-\mathbf{b}d^*_{joint} - \mathbf{t}r_2^b} + (1-f_{joint}) e^{-\mathbf{b}d} \big(\nu^* e^{-\mathbf{t}r_2^b} + (1-\nu^*) e^{-\mathbf{t}r_2^t} \big) \big] \tag{6}$$

2.5 Model Simulations

Model simulations are carried out with distributions of modified parameters to ensure test parameters fall in a sensible range. The model is re-parameterised to ensure that the parameters of interest are constrained to be within physically plausible ranges. Specifically, if D is Gaussian distributed then $d = e^D$ is subject to $d > 0$ (similarly for r_2^b and r_2^t), and for f_{joint}; if F is Gaussian distributed then $f_{joint} = e^F/(1+e^F)$ is subject to $0 \leq f_{joint} \leq 1$ and similarly for ν^*. Ground truth samples are drawn from the distributions of F, D, *et al* and used to generate signal curves with different levels of Gaussian noise added; we then fit directly (non-linear least squares) for the modified parameters. We test 2500 samples for each simulation and each value of SNR between 0.5 and 16 and compare the

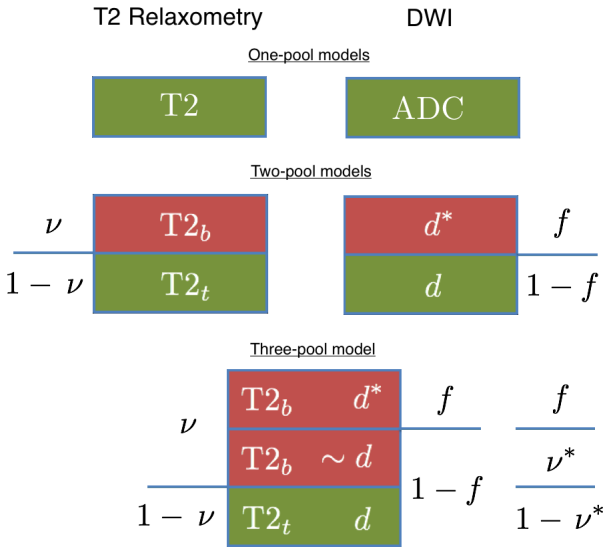

Fig. 1. Taxonomy of multi-component representations of the diffusion and T2 relaxometry signals. Top row: 'single-component' models of ADC and T2 decay (see equations 1 and 2). Middle row: two-component models for IVIM and T2 relaxometry (see equations 4 and 5). Bottom row: combined model of diffusion and T2 relaxation characteristics with volume fractions labelled (see equation 6).

model-fit residuals and parameter-difference vectors. Parameters are initialised with mean $\theta = [S_0 = 0.5, f_{joint} = 0.4, \nu^* = 0.25, d^*_{joint} = 0.023mm^2s^{-1}, d = 0.00185mm^2s^{-1}, r_2^b = (290ms)^{-1}, r_2^t = (46ms)^{-1}]$ [10, 5]. Modified parameters are drawn from normal distributions with unified standard deviation $N(\theta, 0.25)$, the physical values of the relaxivities and diffusivities makes this reasonable. All seven parameters are fitted simultaneously in this section.

We test the following three combinations of data:

1. Using the b-values and TEs described for the separate IVIM and relaxometry volunteer data above, we investigate the influence of adding further multi-TE images at single low b-value at each of: $b = [0, 25, 50, 100, 200, 400, 1000]s.mm^{-1}$.
2. The same set of parameters, b-values and TEs as in simulation 1, but with fixed $\nu^* = 0$.
3. As in simulation 1, but with increased b-value resolution, using initial IVIM experimental values of b=$[0, 25, 50, 75, 100, 125, 150, 200, 400, 600]s.mm^{-1}$ in the simulation.

3 Results

3.1 Results from Model Simulations

Figure 2a shows the influence, at varying SNR, of including low b-value, multi-echo time data on the model fit residual. The model fit residual depends monotonically on the SNR. SNR values greater than 10 would be typical of this type of clinical acqusition. Figure 2b shows the effect of low-b-value, multi TE data on the modified parameter residual: $||\theta_{fit} - \theta_{true}||_2^2$. Summarising the parameter value in this way is acceptable due to the nature of the logarithmically transformed coordinates, values of F,D *et al* have comparable magnitude values. Low b-value multi-TE data in the range $100 - 200 s.mm^{-2}$ allow improved fitting for reasonable SNR. Parameter residuals for either high b-value multi-TE or for b=0 do not confer this same advantage due to loss of signal and insufficient flow suppression respectively. Figure 2c is comparable to Figure 2b but for the case $\nu^* = 0$ representing a system with a single IVIM blood pool; the low b-value, multi-TE data continues to allow more accurate fitting. Figure 2d is comparable to Figure 2b, but in this instance a finer range of b-values have been acquired and the experiment repeated, suggesting that the additional relaxometry data is providing an advantage regardless of the finer range of b-values. These results suggest that mixed low-value b-value multi-TE data is necessary to accurately fit the model (6), but that the b-value is fairly non-specific in the range $50 - 200 s.mm^{-2}$.

3.2 Placenta imaging

We fit the general models above to our placenta dataset. Figure 3 shows parametric maps in the placenta for conventional MRI parameters estimated using Equation 3. Average ($\pm$ standard deviation) T2 values in this ROI are $157 \pm 34 ms$ and average ADC is $0.0018 \pm 0.0001 mm^2 s^{-1}$. Figure 4 compares parameter values between standard IVIM and the joint signal model described in Equation 6 The joint model parameter for the vascular density f has less noisy model fits in general and fits smoothly to the region of amniotic fluid (although notionally this region is not flowing, fetal motion is likely to introduce unpredictably high values for the pseudo-diffusivity). The myometrium is clearly seen with high values of f obtained with both models. Values of f are notably lower in the placenta, suggesting that T2 effects become notable during the joint fitting. Maps of pseudo-diffusivity take on the expected nosy parameter values for both models. ADC (d) maps are comparable for both methods. The introduction of a parametric map of $(1-f)\nu$ allows a new contrast to be obtained in the placenta, providing clear parametric separation between the fetal brain, amniotic fluid and regions of the placenta. IVIM estimates for f_{ivim} and d_{ivim} are 0.24 ± 0.02 and $0.0016 \pm 0.0001 mm^2 s^{-1}$ respectively. For the joint model, parameter estimates for f_{joint}, ν^* and d are 0.09 ± 0.03, 0.23 ± 0.09 and $0.0017 \pm 0.0001 mm^2 s^{-1}$ respectively. These values are plausible for the expected range for this experiment at 1.5T [5].

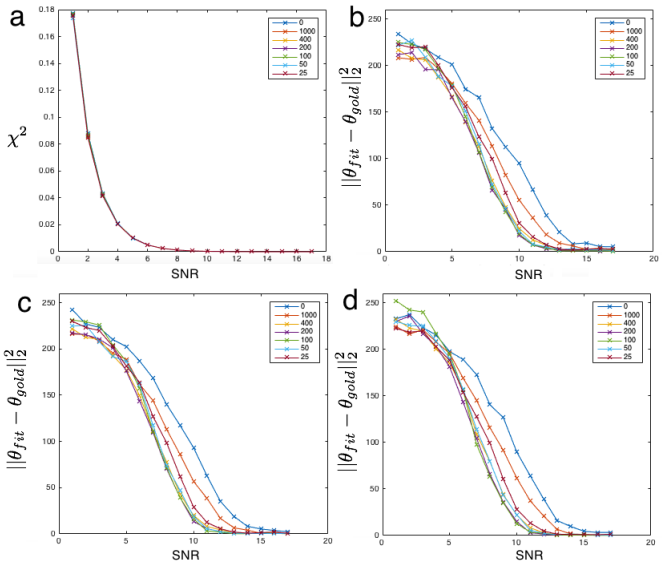

Fig. 2. Effect of data acquisition on model fit parameter accuracy. a) data residual for varying SNR b) Parameter error for $\nu^* > 0$ c) Parameter error for $\nu^* = 0$. d) Parameter error for $\nu^* > 0$ with more finely spaced b-values (see text). Coloured curves correspond to the inclusion of multi-TE data acquired with each b-value.

4 Discussion

The multi-modal data presented in this work have allowed a new model to be applied to combined perfusion (IVIM-like), diffusion and relaxometry images. The acquired data itself represents a novel acquisition, making use of combined multi-echo and variable b-value data and using variable TR. Simulations showed that parameter estimation is aided by the combination of mixed echo-time and diffusion weighting. Although in this work, the joint model fitting was used in only one application, there are several other abdominal organs which may make use of this technique; for instance within the kidney the joint model-fitting could also have potential to aid existing multi-compartment models [11] (this is particularly interesting given the parametric separation of medullary and central-kidney flow regimes). Within the placenta the short acquisition time could have a significant clinical utility in assessing pathological placental growth and assessing the need for future intervention in conditions such as twin-twin transfusion syndrome.

Currently our work is limited by a fixed b-value step size of $50 s.mm^{-2}$ and by the requirement of assuming fixed compartmental T2s but the model-fitting helps to mitigate this feature. In future we plan to acquire more placental data, this generalisation of this analysis is limited by application to a single case,

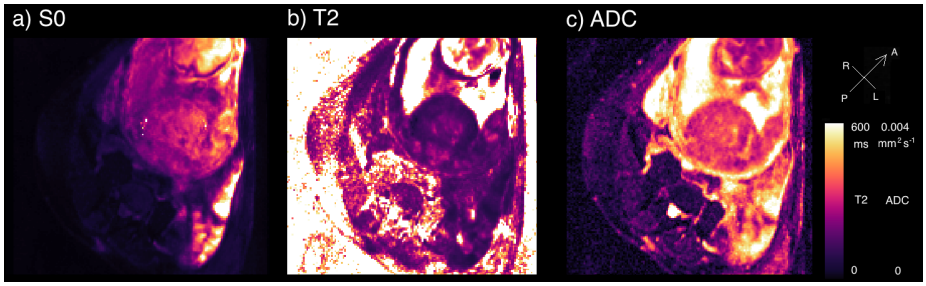

Fig. 3. Parametric maps in the placenta for the model described in Equation 3: Estimates for the initial signal magnitude S0, T2 (ms) and ADC (mm^2s^{-1}) respectively.

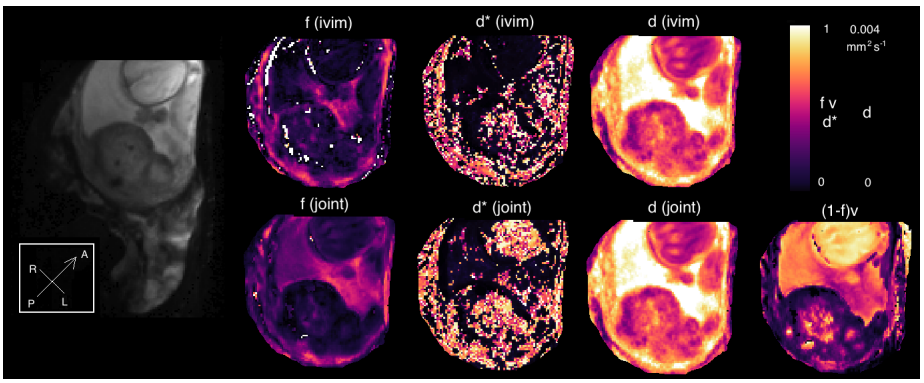

Fig. 4. Parametric maps in the placenta: top row, standard IVIM parameter estimates for the vascular density f, pseudo-diffusivity, d^*, and ADC, d (Equation 4). Bottom row: joint model estimates for vascular density, f, pseudo-diffusivity, d^*, ADC and static-fluid fraction, $(1-f)\nu$ (Equation 6).

and test a comparable acquisition at 3T. This may enable us to obtain data of sufficient SNR and allow free fitting of the full 7-parameter model, avoiding the use of literature values for the tissue relaxivities. We also intend to acquire more data to explore the clinical utility of this extended diffusion models and assess its suitability for placental imaging across a range of twin-twin transfusion cases.

Future work will also assess how tolerant the model-fitting procedure is of missing or motion-corrupted data, for instance by using a model-selection procedure. This is particularly relevant for the placental image analysis. However the acquisition has been designed to be quite robust since parameters such as the ADC and the T2 can be estimated from only a few acquired images from the beginning of the acquisition; acquiring more variable TE and b-value imaging data allows the fitting of more sophisticated two and three compartment models and tissue and flow related volume fractions.

To further validate this work, it is possible to mathematically model the effects of tissue structure on perfusion using a suitable analogous model such as [12]. Complementary imaging contrasts could also be used to understand more deeply the placenta and abdominal organ function [13].

In summary, we have developed a bespoke abdominal acquisition and multi-compartment model that can be used to reveal new features about abdominal organs by making use of combined relaxometry and diffusion weighted MRI. The novel acquisition of combined diffusion and multi-echo T2 imaging within clinically feasible time frames in this work will allow us to investigate new biomarkers and to generate novel predictive measurements of tangible physical parameters.

Acknowledgements We would like to acknowledge the MRC (MR/J01107X/1), the National Institute for Health Research (NIHR), the EPSRC (EP/H046410/1) and the National Institute for Health Research University College London Hospitals Biomedical Research Centre (NIHR BRC UCLH/UCL High Impact Initiative BW.mn.BRC10269). This work is supported by the EPSRC-funded UCL Centre for Doctoral Training in Medical Imaging (EP/L016478/1).

References

1. Gowland, P.: Placental mri. Semin Fetal Neonatal Med **10**(5) (Oct 2005) 485–490
2. Chalouhi, G.E., Deloison, B., Siauve, N., Aimot, S., Balvay, D., Cuenod, C.A., Ville, Y., Clment, O., Salomon, L.J.: Dynamic contrast-enhanced magnetic resonance imaging: definitive imaging of placental function? Semin Fetal Neonatal Med **16**(1) (Feb 2011) 22–28
3. Siauve, N., Chalouhi, G.E., Deloison, B., Alison, M., Clement, O., Ville, Y., Salomon, L.J.: Functional imaging of the human placenta with magnetic resonance. Am J Obstet Gynecol **213**(4 Suppl) (Oct 2015) S103–S114
4. Le Bihan, D., Breton, E., Lallemand, D., Aubin, M.L., Vignaud, J., Laval-Jeantet, M.: Separation of diffusion and perfusion in intravoxel incoherent motion mr imaging. Radiology **168**(2) (Aug 1988) 497–505
5. Derwig, I., Lythgoe, D.J., Barker, G.J., Poon, L., Gowland, P., Yeung, R., Zelaya, F., Nicolaides, K.: Association of placental perfusion, as assessed by magnetic resonance imaging and uterine artery doppler ultrasound, and its relationship to pregnancy outcome. Placenta **34**(10) (Oct 2013) 885–891
6. Derwig, I., Barker, G.J., Poon, L., Zelaya, F., Gowland, P., Lythgoe, D.J., Nicolaides, K.: Association of placental t2 relaxation times and uterine artery doppler ultrasound measures of placental blood flow. Placenta **34**(6) (Jun 2013) 474–479
7. Melbourne, A., Atkinson, D., White, M.J., Collins, D., Leach, M., Hawkes, D.: Registration of dynamic contrast-enhanced mri using a progressive principal component registration (ppcr). Phys Med Biol **52**(17) (Sep 2007) 5147–5156
8. Modat, M., Ridgway, G., Taylor, Z., Lehmann, M., Barnes, J., Hawkes, D., Fox, N., Ourselin, S.: Fast free-form deformation using graphics processing units. Computer methods and programs in biomedicine (Oct 2010)
9. MacKay, A., Laule, C., Vavasour, I., Bjarnason, T., Kolind, S., Mdler, B.: Insights into brain microstructure from the t2 distribution. Magn Reson Imaging **24**(4) (May 2006) 515–525

10. Stanisz, G.J., Odrobina, E.E., Pun, J., Escaravage, M., Graham, S.J., Bronskill, M.J., Henkelman, R.M.: T1, t2 relaxation and magnetization transfer in tissue at 3t. Magn Reson Med **54**(3) (Sep 2005) 507–512
11. Notohamiprodjo, M., Chandarana, H., Mikheev, A., Rusinek, H., Grinstead, J., Feiweier, T., Raya, J.G., Lee, V.S., Sigmund, E.E.: Combined intravoxel incoherent motion and diffusion tensor imaging of renal diffusion and flow anisotropy. Magn Reson Med **73**(4) (Apr 2015) 1526–1532
12. Forsgren, M.F., Dahlqvist Leinhard, O., Dahlstrm, N., Cedersund, G., Lundberg, P.: Physiologically realistic and validated mathematical liver model reveals [corrected] hepatobiliary transfer rates for gd-eob-dtpa using human dce-mri data. PLoS One **9**(4) (2014) e95700
13. Huen, I., Morris, D.M., Wright, C., Parker, G.J.M., Sibley, C.P., Johnstone, E.D., Naish, J.H.: R1 and r2* changes in the human placenta in response to maternal oxygen challenge. Magn Reson Med **70**(5) (Nov 2013) 1427–1433